Water Resources Research

Supporting Information for

Streamflow intermittence in Europe: Estimating high-resolution monthly time series by downscaling of simulated streamflow and Random Forest modeling

Petra Döll1[1,2*], Mahdi Abbasi[1*], Mathis Loïc Messager[3,4], Tim Trautmann[1], Bernhard Lehner[4], Nicolas Lamouroux[3]

[1]Institute of Physical Geography, Goethe University Frankfurt, Frankfurt/Main, Germany, [2]Senckenberg Leibniz Biodiversity and Climate Research Centre (SBiK-F) Frankfurt, Frankfurt/Main, Germany, [3]INRAE, UR RiverLy, Lyon-Villeurbanne, France, [4]Department of Geography, McGill University, Montreal, Canada

Corresponding author: Petra Döll (p.doell@em.uni-frankfurt.de)

*Equal contribution

Contents of this file

Text S1. Further adjustments of the correction factor used in the downscaling algorithm

The correction factor C_{Li} (Equation 2) is augmented for certain grid cells as explained below.

S1.1 Redistribution of water storage modifications in large lakes and reservoirs

In WaterGAP, reservoirs with a maximum storage capacity of at least 0.5 km³, regulated lakes with a maximum storage capacity of at least 0.5 km³ or an area of more than 100 km², and lakes with a minimum area of 100 km² are considered as so-called 'global surface water bodies' (Müller Schmied et al., 2021) that receive water not only from the surface runoff and groundwater discharge generated within the LR cell but also from upstream streamflow. Global surface water bodies may spread over more than one LR grid cell and their overall water balance is calculated in their assigned outflow cell. Thus, the initial net cell runoff (ncR_{Li}) of this outflow grid cell includes the runoff generated by the global surface water bodies (a single grid cell may represent the outflow of multiple global surface water bodies), which needs to be redistributed to all LR grid cells that intersect with these global surface water bodies and their respective HR cells. This is done by calculating the change of water storage in the global surface water body for each month compared to the previous month. This amount is subtracted from the net cell runoff of the outflow cell and redistributed in an area-weighted way to all upstream LR cells intersecting one of the global surface water bodies. Every LR cell has its net cell runoff from global surface water bodies assigned based on the area of the cell that intersects the global surface water body. Then these LR values are applied to those HR cells that are covered by polygons of global surface water bodies. As HR grid cells have different grid cell areas, the distribution of runoff from global surface water bodies is area-weighted.

S1.2 Additional correction for remaining discrepancies in large rivers

Routing in WaterGAP is performed along the 0.5 arc-deg DDM30 river network (Döll & Lehner, 2002), but HR streamflow is computed based on a slightly modified version of the 15 arc-sec river network of HydroSHEDS (Lehner et al., 2008). Given their different spatial resolutions and generation processes, these two river networks differ locally in their representation of river courses and related characteristics. This, in turn, may cause the correction term C_{Li} (Eq. 2) to not take effect in the desired way. One major issue is that the HydroSHEDS river network contains additional endorheic sinks, typically smaller ones, that are not covered by the DDM30 river network. Endorheic sinks (or depressions) are basins without an outlet to the ocean, represented topographically by one or multiple grid cells that are surrounded by higher elevation values. Those local endorheic sinks are not covered by the LR DDM30 because they occur at a smaller geographic scale that cannot be represented by the LR (0.5 arc-deg) grid cells. In such cases, for example if a subgrid endorheic sink covers half of an LR cell, the initial correction term C_{Li} would be applied to all HR cells in the LR cell. But in the subsequent routing of discharge along HR grid cells, the discharge within the endorheic sink would not contribute to the discharge of the mainstem river, and thus the original C_{Li} term alone would not be capable to correct the mainstem's flow quantities.

An additional correction mechanism, already included in the original method of Lehner and Grill (2013), aims at correcting for such HR endorheic sinks but also covers other remaining artefacts that cause deviations between LR and HR streamflow estimates. Importantly, this additional correction mechanism is only applied to relatively large rivers, i.e., those with an upstream area of at least 50,000 km², and for locations with a reasonable accordance in drainage areas between DDM30 and HydroSHEDS: for rivers with catchment areas between 50,000 and 100,000 km^2, they are allowed to differ by up to 20%, and for rivers with catchment areas of >100,000 km^2, they are allowed to differ by up to 50%. These criteria are necessary because the two river networks can diverge strongly at local scale, especially in headwater areas and at confluences. For example, an HR grid cell may represent only a tributary to a mainstem, whereas the corresponding LR grid cell from DDM30 may represent the (much larger) mainstem. Therefore, if the above conditions are not fulfilled, additional corrections could cause major deteriorating effects on the results.

For those LR cells that fulfill the above criteria, the initial correction term $C_{Li,init}$ (Eq. 2) is extended by an additional correction term. This modification of the correction term C_{Li} is calculated by comparing the net cell runoff of the LR cell with the net cell runoff of the HR grid cell with the maximum upstream area in that LR cell, with

$$C_{Li} = C_{Li,init} + (ncR_{Li}^{LR} - ncR_{Li}^{HR}) \quad \text{(S1)}$$

The HR net cell runoff representation of LR grid cell L_i (ncR_{Li}^{HR}) is calculated as the streamflow of the HR grid cell with the maximum upstream area in L_i ($Q_{Li,Hj}$; Eq. 1) minus the corresponding streamflow values of direct upstream LR grid cells.

S1.3 Equalizing correction terms by partially shifting them to the next downstream LR grid cell

The additional correction term (see S1.2) can introduce correction gaps caused by discrepancies between the DDM30 and HydroSHEDS river networks. These gaps can then lead to oscillating upward and downward corrections in neighboring LR grid cells. To smooth such oscillating corrections, the correction terms are partially propagated to the next downstream LR grid cell and are thus balanced with the correction term in that cell. The partial shifts of the correction terms along the LR river network are only applied if the maximum HR upstream area in the downstream LR cell is at least 90% of that in the evaluated LR cell. This criterion guarantees that the correction values are solely shifted to larger streams (within a 10% tolerance to consider minor discrepancies such as endorheic sinks) and that shifting between LR cells with mismatching river networks is avoided. The fraction of the correction term that is shifted downstream depends on the difference between upstream and downstream basin area such that 50% of the correction term is shifted downstream if the two neighboring cells represent equal basin size (i.e., along the same river), and an increasingly higher fraction is shifted downstream if a smaller river flows into a larger one (as applying a correction in a larger river leads to less potential distortion). The fractional shift is computed as

$$fr_{Li}^{shift} = \begin{cases} \dfrac{(2 * upA_{Li,down}^{Max} - upA_{Li}^{Max})}{2 * upA_{Li,down}^{Max}}, & upA_{Li,down}^{Max} > 0.9 \ * \ upA_{Li}^{Max} \\ 0, & upA_{Li,down}^{Max} \leq 0.9 \ * \ upA_{Li}^{Max} \end{cases} \qquad \text{(S2)}$$

with $upA_{Li,down}^{Max}$ representing the maximum HR upstream area in the downstream LR grid cell and upA_{Li}^{Max} representing the maximum HR upstream area in the evaluated LR grid cell L_i. Following this approach, the modified correction term for a given LR grid cell L_i consists of the part which is not shifted downstream and the parts which originate from the shifted correction terms from direct upstream cells $C_{Li,upj}$.

$$C_{Li} = C_{Li,init} * \left(1 - fr_{Li}^{shift}\right) + \sum_{j=1}^{n} (C_{Li,upj} * fr_{Li,upj}^{shift}) \qquad \text{(S3)}$$

S1.4 Negative and extreme correction values

Despite the various correction and balancing algorithms described above, it is possible that in singular cases negative values of streamflow or extreme correction values are calculated. This can happen, for example, in places where there are major discrepancies between the LR and HR river network alignments or where their upstream areas differ substantially. Three measures are sequentially implemented to limit potential artefacts caused by applying the final correction term. First, the final correction term is limited to a maximum threshold value of 0.001 $m^3 s^{-1}$ per km^2 of upstream area. Second, any negative HR streamflow values, which may originate from side effects of the correction mechanisms, are not accumulated along the river network. A negative streamflow value can turn positive during flow accumulation if streamflow is added from upstream cells, but negative correction values are not propagated along the river network. Third, all remaining negative streamflow values are set to zero in the final step.

S1.5 Technical implementation

The software implementation of the downscaling algorithm was developed in Python. A set of Python scripts (with ArcPy dependency) was developed to preprocess necessary static data. The static data listed below are necessary to run the downscaling algorithm.

Data	Description
flow_dir_15s_by_continent.gdb	HydroSHEDS flow directions [ESRI flow direction codes]
pixel_area_skm_15s.gdb	HydroSHEDS area of HR grid cells [km²]
flowdir_30min.tif	DDM30 flow directions [ESRI flow direction codes]
landratio_correction.tif	Ratio between percent of LR cell covered by HydroSHEDS landmask and percent of cell covered by WaterGAP landmask [-]
orgDDM30area.tif	Area of LR cells of WaterGAP [km²]
pixareafraction_glolakres_15s.tif	Ratio of global surface water bodies that is covered by the HR grid cell [-]

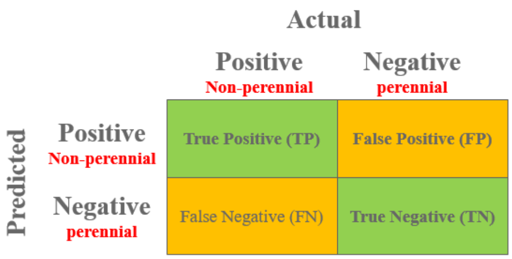

Figure S1. Binary confusion matrix in case of two classes (perennial and non-perennial) only.

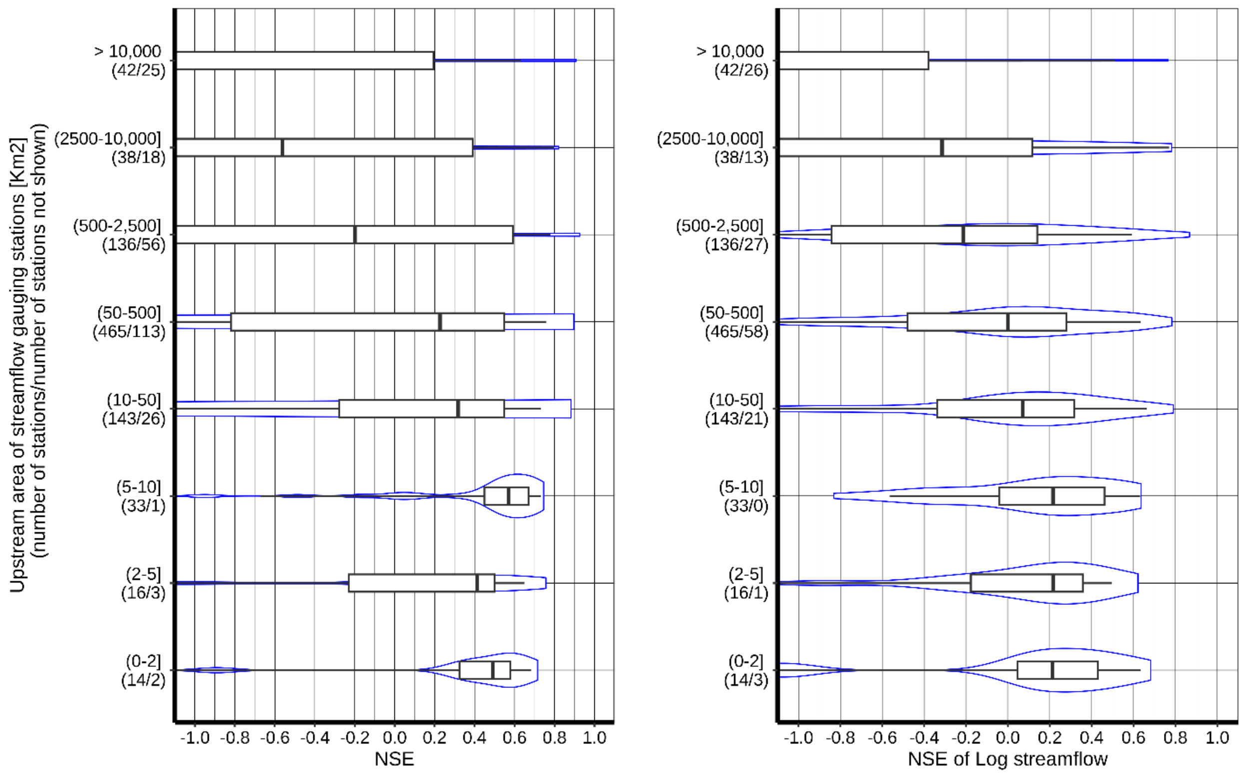

Figure S2. NSE of monthly streamflow time series (left) and of the logarithm of monthly streamflow time series (right) for all 885 intermittent streamflow stations with observations, grouped in size classes of the upstream area of the streamflow gauging stations. The boxes indicate the 25th, 50th (median) and 75th percentiles, the whiskers indicate the 5th and 95th percentiles of the samples. The blue lines of the violin plot show the smoothed distribution of the data points. The “number of stations not shown” indicates the number of stations with an NSE of less than -1.

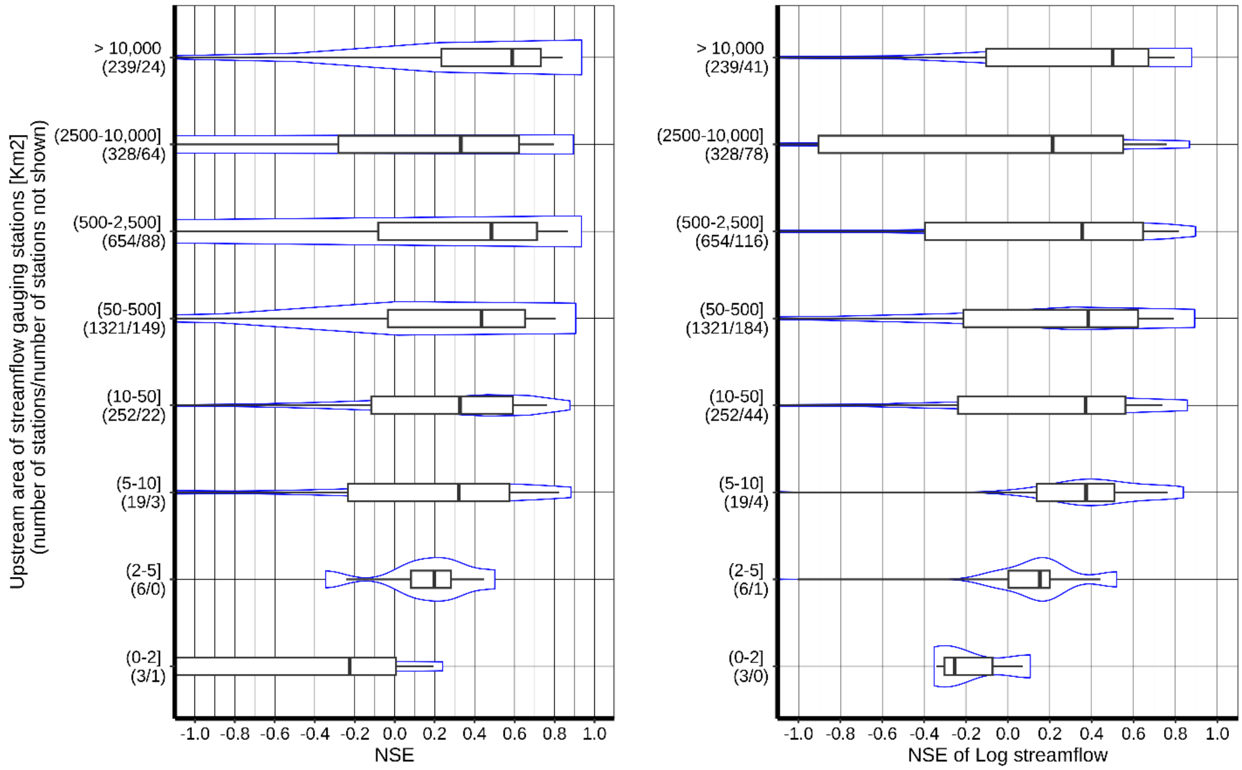

Figure S3. NSE of monthly streamflow time series (left) and of the logarithm of monthly streamflow time series (right) for all 2,821 perennial streamflow stations with observations, grouped in size classes of the upstream area of the streamflow gauging stations. The boxes indicate the 25th, 50th (median) and 75th percentiles, the whiskers indicate the 5th and 95th percentiles of the samples. The blue lines of the violin plot show the smoothed distribution of the data points. The "number of stations not shown" indicates the number of stations with an NSE of less than -1.

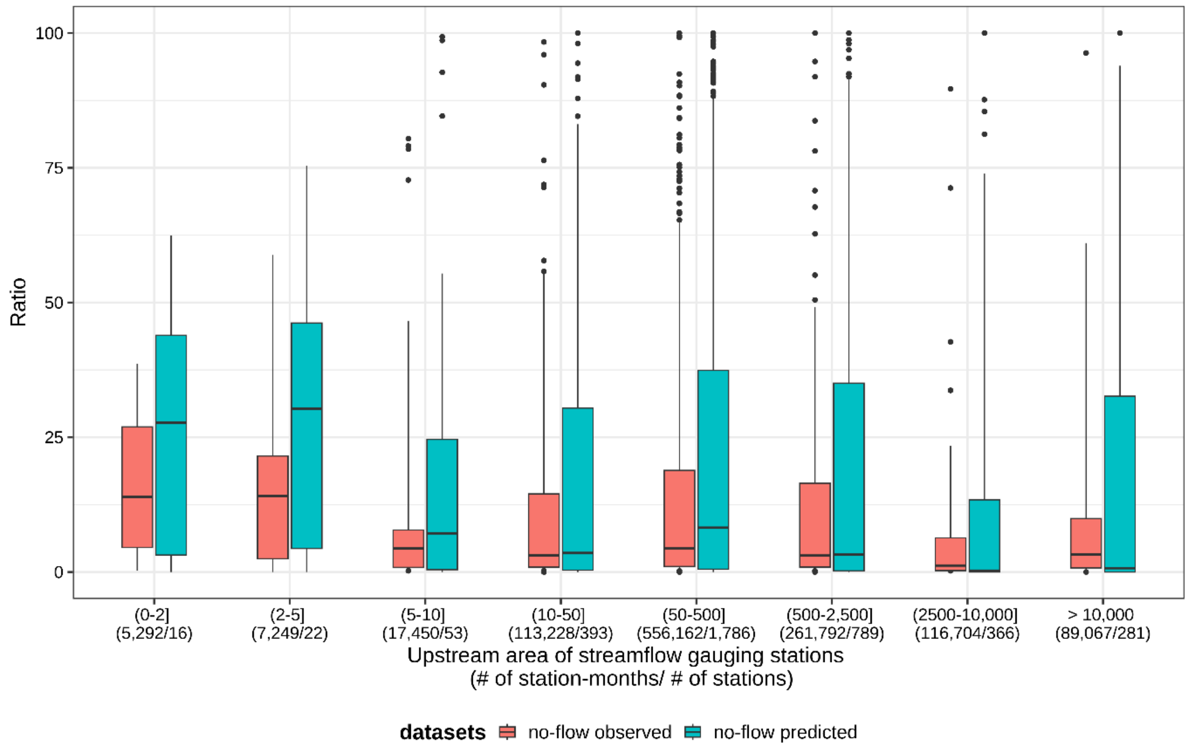

Figure S4. Performance of the step 1 RF as a function of upstream drainage area [km^2] of the streamflow gauging stations. The box plot shows the percent of all station-months in a drainage area class that are observed (red) or simulated (green) as intermittent. The values below the upstream area show the number of station-months/number. The boxes indicate P25 (25th percentile), P50 (median) and P75, the whiskers P5 and P95 of the samples.

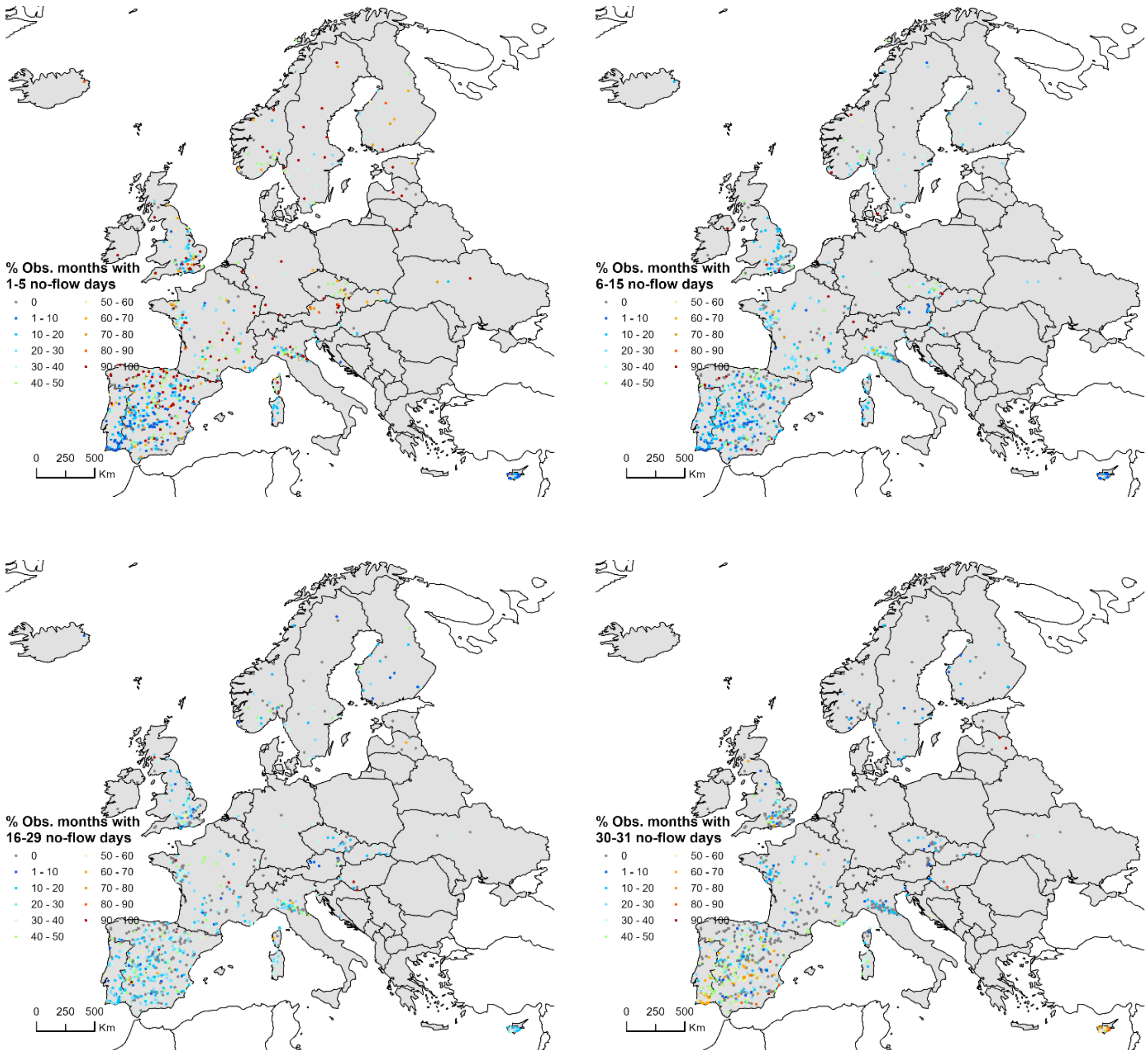

Figure S5. Percentage of intermittent months with observations of the four intermittence classes (1-5, 6-15, 16-29, 30-31 no-flow days per month) at gauging stations in the complete streamflow dataset.

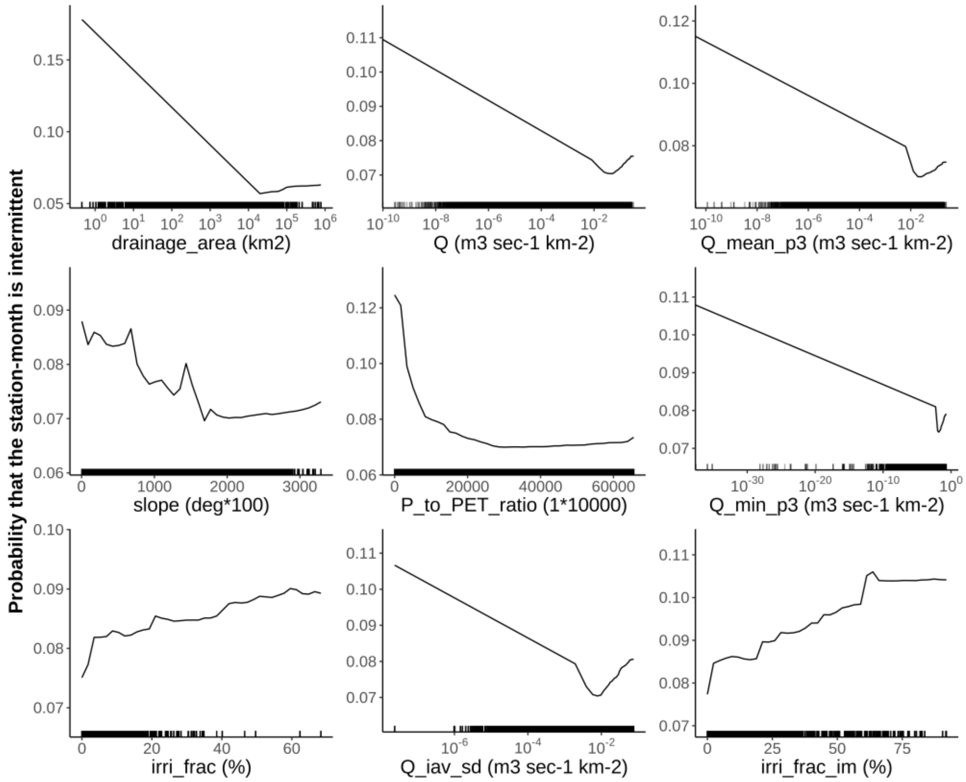
Probability that the station-month is intermittent
drainage_area (km2)
Q (m3 sec-1 km-2)
Q_mean_p3 (m3 sec-1 km-2)
slope (deg*100)
P_to_PET_ratio (1*10000)
Q_min_p3 (m3 sec-1 km-2)
irri_frac (%)
Q_iav_sd (m3 sec-1 km-2)
irri_frac_im (%)

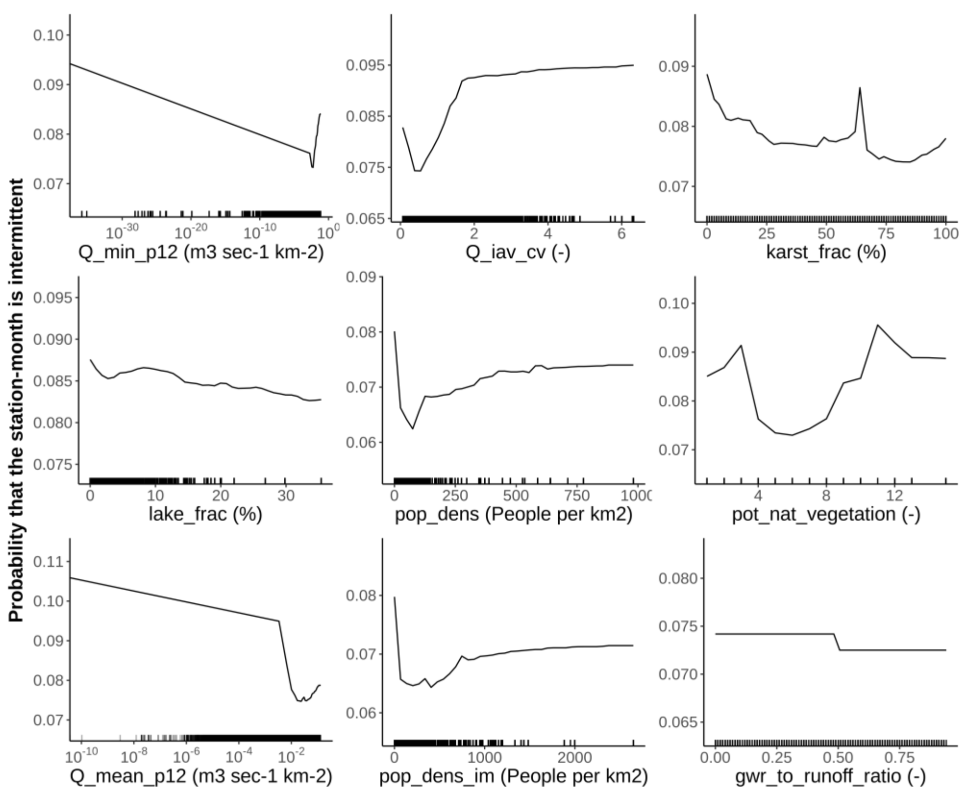
Probability that the station-month is intermittent
Q_min_p12 (m3 sec-1 km-2)
Q_iav_cv (-)
karst_frac (%)
lake_frac (%)
pop_dens (People per km2)
pot_nat_vegetation (-)
Q_mean_p12 (m3 sec-1 km-2)
pop_dens_im (People per km2)
gwr_to_runoff_ratio (-)

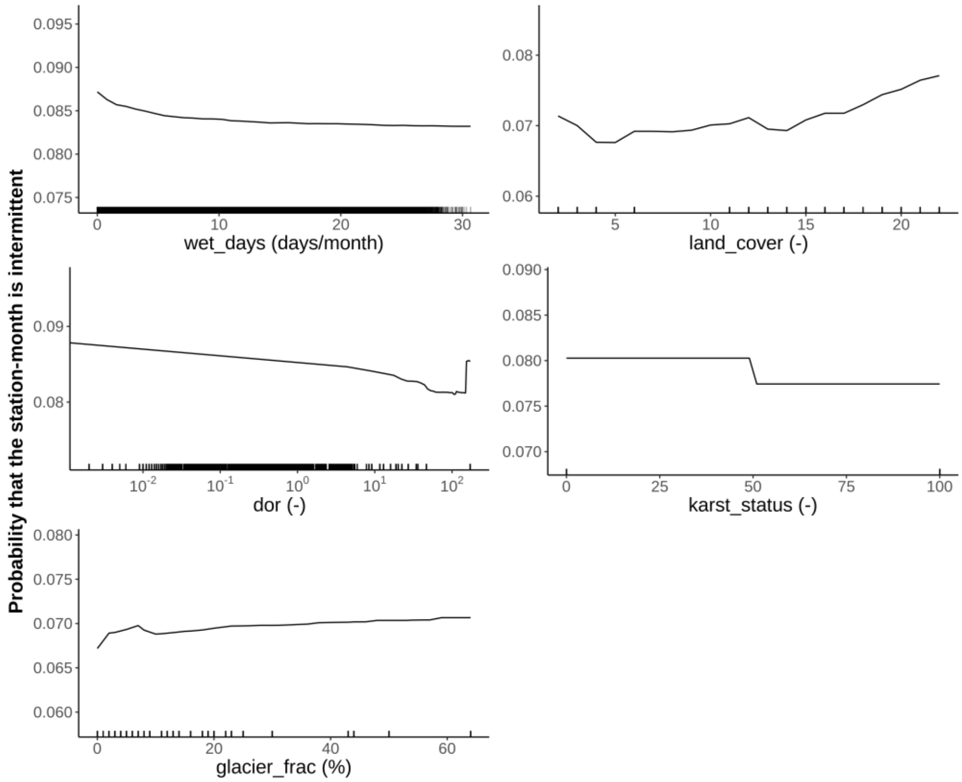

156 **Figure S6.** Partial dependence plots for the 23 predictors of the step 1 RF.

157

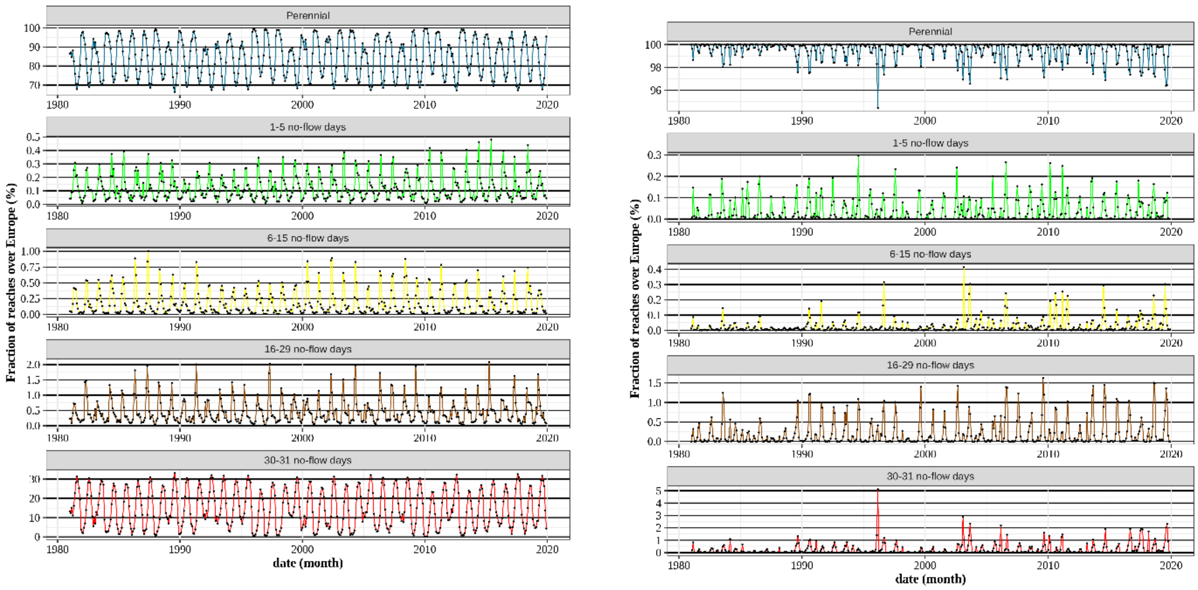

Figure S7. Monthly time series of the percent of reaches in the five intermittence classes in southern Europe (Portugal Spain, Italy, Greece and Cyprus) (left) and in Scandinavia (Norway, Sweden and Finland (right).

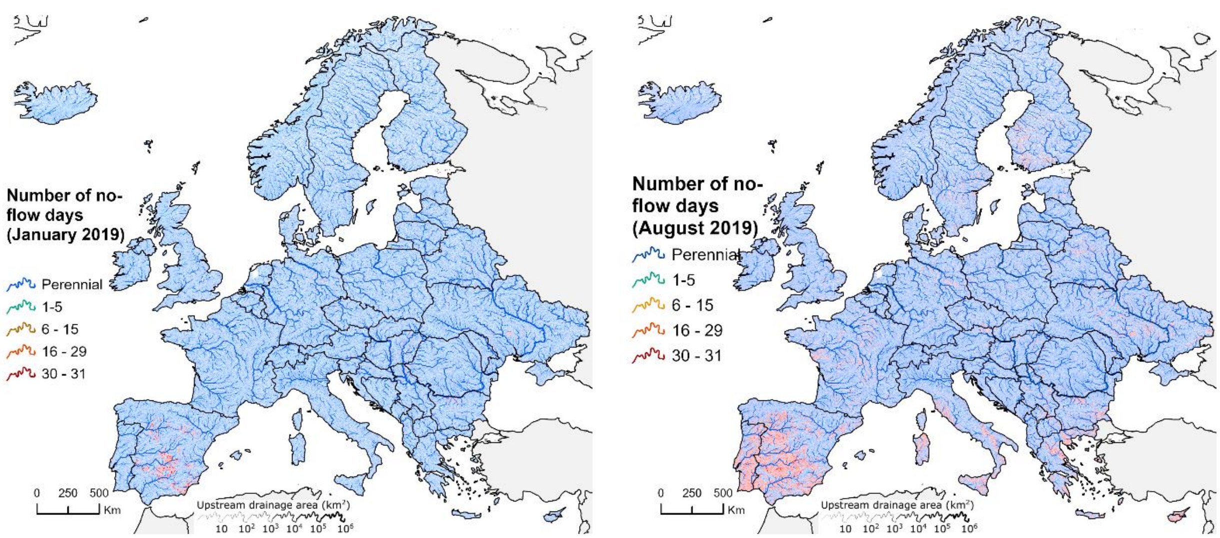

Figure S8. Number of no-flow days, in five classes, in January 2019 (left) and August 2019 (right).